Environment Protection Engineering

Vol. 1 1975 No. 1

HILARY FIREWICZ, ROMAN KOCH*

THE MECHANISM OF GRANULAR SOLID FLOW IN A VERTICAL PULSE COLUMN FOR THE LIQUID-SOLID SYSTEMS

An apparatus for continuous counter-current liquid/solid transport, based on a pulsing flow of the liquid has been discussed. The equation describing this model have been confirmed by results obtained from the experiment performed on semi-industrial scale. An additional empirical relation between the mean velocity of the shift of the particles $(n \cdot C_L)$ and the mass flow rate of granular solid $((\dot{m}_s)_{\max})$ has been obtained. The arguments speaking for the assumed model have been also given. In order to avoid possible side – effects on the solid flow through the pulse column the investigations have been performed on model systems; the components used were chemically neutral and showed neither agglomeration nor dissolution tendencies.

NOMENCLATURE

A – The amplitude of the pulsation of liquid column in the apparatus, m; amplituda pulsacji mierzona w kolumnie;

C_L – Constant, m; stała wymiarowa;

d_p – (Substitute) diameter of the solid particles, m; średnica (zastępcza) ziaren ciała stałego; m_z,

H – Height of the bed in the downcomer (Fig. 3), m; wysokość złoża w przelewie (rys. 3);

* H. FIREWICZ – Assistant professor, R. KOCH – Professor, Institute of Chemical Engineering and Heating Equipment Wrocław Technical University, Wrocław, Poland.

l – Submersion height of the downcomer (Fig. 3), m;
wysokość zanurzenia przelewu (rys. 3);

L – Distance covered by the particle, approximately equal to the distance between the downcomers (Fig. 3), m;
odległość, jaką przebywa cząstka na półce w przybliżeniu równa odległości między przelewami (rys. 3);

$\dot{m}_s$ – Mass flow rate of the solid referred to the dry granular material, kg/s, g/s;
masowe natężenie przepływu fazy stałej, odniesione do suchego materiału ziarnistego;

$(\dot{m}_s)_{\max}$ – Maximum mass permissible flow rate of the solid;
maksymalne masowe natężenie przepływu fazy stałej graniczące z zasypywaniem przelewu;

$\frac{(\dot{m}_s)_{\max}}{F}$ – Mass velocity of the granular solid, referred to one square metre of cross-section area of the downcomer, $kg/m^2\,s$;
prędkość masowa rozdrobnionego ciała stałego, odniesiona do jednego metra poprzecznej powierzchni przelewu;

n – Pulsation frequency or rotational speed of the pulsator, n 1/s, cycles/min;
częstotliwość pulsacji lub obroty pulsatora;

$n \cdot C_L$ – Velocity of the solid movement along the tray, when F_r is the front surface, m/s;
prędkość przesuwu ciała stałego wzdłuż półki, gdy powierzchnią czołową jest powierzchnia F_r;

F – Cross-section of the downcomer (Fig. 5), m^2;
powierzchnia poprzeczna przelewu;

F_r – Rectangular area below the downcomer, constituting the front surface, perpendicular to the direction at which the granular material moves along the tray (Fig. 5), m^2;
powierzchnia pod przelewem, prostopadła do kierunku ruchu materiału ziarnistego na półce;

T – Duration of one cycle of the pulsator, s;
okres cyklu pulsatora;

w_l – Velocity of the liquid, m/s;
prędkość cieczy;

$w_l(\tau)$ – Momentary (cummulative – total) velocity of the liquid in the column, m/s;
chwilowa (sumaryczna) prędkość cieczy w kolumnie;

w_{mf} – Minimum fluidizing velocity (incipient fluidization), m/s;
prędkość krytyczna (początek fluidyzacji);

w_t – Teminal free-falling velocity of a particle, m/s;
prędkość opadania pojedynczej cząstki ;

w_{fl} – Liquid flow velocity resulting from the actual (real) liquid flow rate in the column, m/s;
prędkość przepływu cieczy, wynikająca z rzeczywistego natężenia przepływu cieczy w kolumnie;

w_{puls} – The component of liquid flow velocity resulting from the reciprocal motion of the piston, m/s;
składowa prędkości cieczy, wynikająca z posuwisto-zwrotnego ruchu tłoka;

x – Exponent (power index) in the simplified Zaki-Richardson equation; wykładnik potęgowy w uproszczonym równaniu Zaki-Richardsona;

$(\overline{\Delta\varrho_{sp}})_a$ – Average difference in the suspension and liquid densities, calculated from eq. (22), kg/m^3; średnia różnica gęstości zawiesiny ciała stałego i cieczy, obliczona z równania (22)

$\Delta\varrho_{sp}(\tau)$ – Momentary difference in the suspension and liquid densities, kg/m^3; chwilowa różnica gęstości zawiesiny ciała stałego i cieczy;

ε_{mf} – Porosity of the bed at the incipient fluidization; porowatość złoża w punkcie krytycznym fluidyzacji;

ε_{min} – Minimum porosity of the bed at the O.D.C position of the piston; najmniejsza porowatość, jaką osiąga złoże, gdy tłok znajduje się w D.M.P.;

$\varepsilon(\tau)$ – Momentary porosity of the bed on the tray; porowatość chwilowa złoża na półce;

η_l – Dynamic coefficient of the liquid viscosity; $(N \cdot s)/m^2$; dynamiczny współczynnik lepkości cieczy;

ϱ_l – Density of the liquid, kg/m^3;. gęstość cieczy;

ϱ_s – Density of the solid, kg/m^3; gęstość ciała stałego;

$(\varrho_{sp})_{max}$ – Maximum densities of the suspension in the downcomer or in the tray at the O.D.C. of the piston, kg/m^3; gęstość maksymalna zawiesiny ciała stałego i cieczy w przelewie lub na półce, gdy tłok znajduje się w D.M.P.;

$\varrho_{sp}(\tau)$ – Momentary densities of the suspension on the tray, kg/m^3; gęstość chwilowa zawiesiny ciała stałego i cieczy na półce;

τ – Time, s; czas.

INDICES

s – solid (ciało stałe);
l – liquid (ciecz);
sp – suspension (zawiesina);
a – average (mean) value (średnia wartość).

1. INTRODUCTION

The vertical pulse column, shown schematically in Fig. 1, is a simple modification of a jigger used for the enrichment of ore. The possibility of applying the jigger to a continuous processes in the system liquid-solid was for the first time suggested by Swinton and Weiss [18, 19]. The jigger modified by Swinton and Weiss ensured a continuous counter-

-current (liquid/solid) flow, avoiding the use of mechanical devices to shift the solid phase. This kind of granular solid flow results from the difference in the densities of granular material and the liquid, as well as from the pulsation flow of liquid caused by the pulsator.

The essential parts of the apparatus are shown in Fig. 1. It consists of a vertical multi-section column (*1*) with downcomers (*2*) and a pulsator (*3*) setting the liquid in reciprocating motion. Under the influence of the pulsing flow of the liquid the granular solid, fed from a storage bin (*4*) to the upper part of the apparatus, moves down the column, from

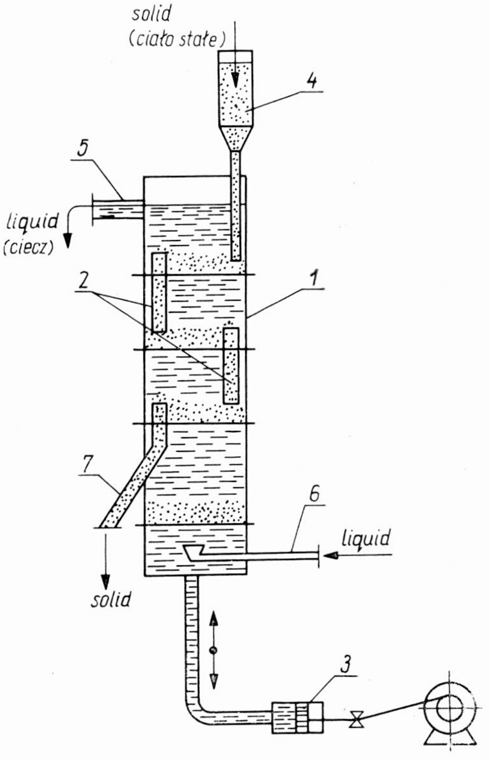

Fig. 1. A scheme of a vertical pulse column for the systems: liquid/solid; *1* — vertical column, *2* — downcomers, *3* — pulsator allowing for the adjustment of pulsation amplitute and frequency, *4* — dispersed solid container, *5* and *6* — outlet/ /inlet pipes for the liquid, *7* — outlet pipe for the solid

Rys. 1. Schemat pionowej kolumny pulsacyjnej dla układu: ciecz—ciało stałe *1* — kolumna pionowa, *2* — przelewy, *3* — pulsator pozwalający na zmianę amplitudy i częstotliwości pulsacji, *4* — zbiornik z rozdrobnionym ciałem stałym — doprowadzenie fazy stałej do kolumny, *5*, *6* — odpowiednio rura odprowadzająca i doprowadzająca ciecz do kolumny, *7* — przewód odprowadzający ciało stałe z kolumny tray to tray, through the succeeding downcomers. This movement of solid is analogical to the flow of a liquid in columns with downcomers, operating in a system gas-liquid. In that case, the liquid being fed to the lower part of the column, flows upwards and most often is discharged through a drain pipe (*5*).

From the data found in the available bibliography [4–7], [11, 12, 15, 16, 17, 18, 19], the following statements may be formulated:

1. A vertical multi-tray pulse column, operating in a continuous counter-current liquid-solid systems makes possible

– to control the contact between the liquid and solid within a sufficiently wade range of time;

– to ensure a uniform flow of a solid and liquid, and consequently, to minimize the channeling and backmixing of both phases.

2. The experiments on the mass exchange [4–6], [11, 12] suggest a considerable usefulness of the above apparatus for the adsorption, ion-exchange and leaching processes.

3. The flow of the solid, is connected with fluidization and has a complex character [5].

4. The results presented in papers [4–6], [11, 12, 18, 19] do not allow to calculate the solid flow rate and the amount of the exchanged component for an arbitrary liquid-solid system.

It follows, moreover, that vertical columns may find wide applications, namely:

a) in power generating industry, in order to obtain the water of high purity at the ion-exchangers;

b) in sugar and pharmaceutical industries for the cleaning and dewatering of the solutions by applying suitable adsorbents;

c) at the recovery of valuable elements (copper, sulphur, precious metals) from all kinds of ores, by means of leching or chemical extraction.

Much attention in the literature is given to the ion-exchange process. E.g. the information on a successful use of a multi-tray pulse column for the softening of water by ion-exchange is given in [6]. The pulse column designed by Grimmett [4, 5] appeared to be highly efficient when applied to the process of ion-exchange. The above observations have been confirmed by the investigations performed on copper-sodium-Dowex 50 and copper-hydrogen-Dowex 50 systems. It has been stated that a column equipped with 3 or 4 trays is sufficient enough to remove the copper from the aqueous solutions.

The above apparatus, despite its usefulness, have not been sufficiently elaborated.

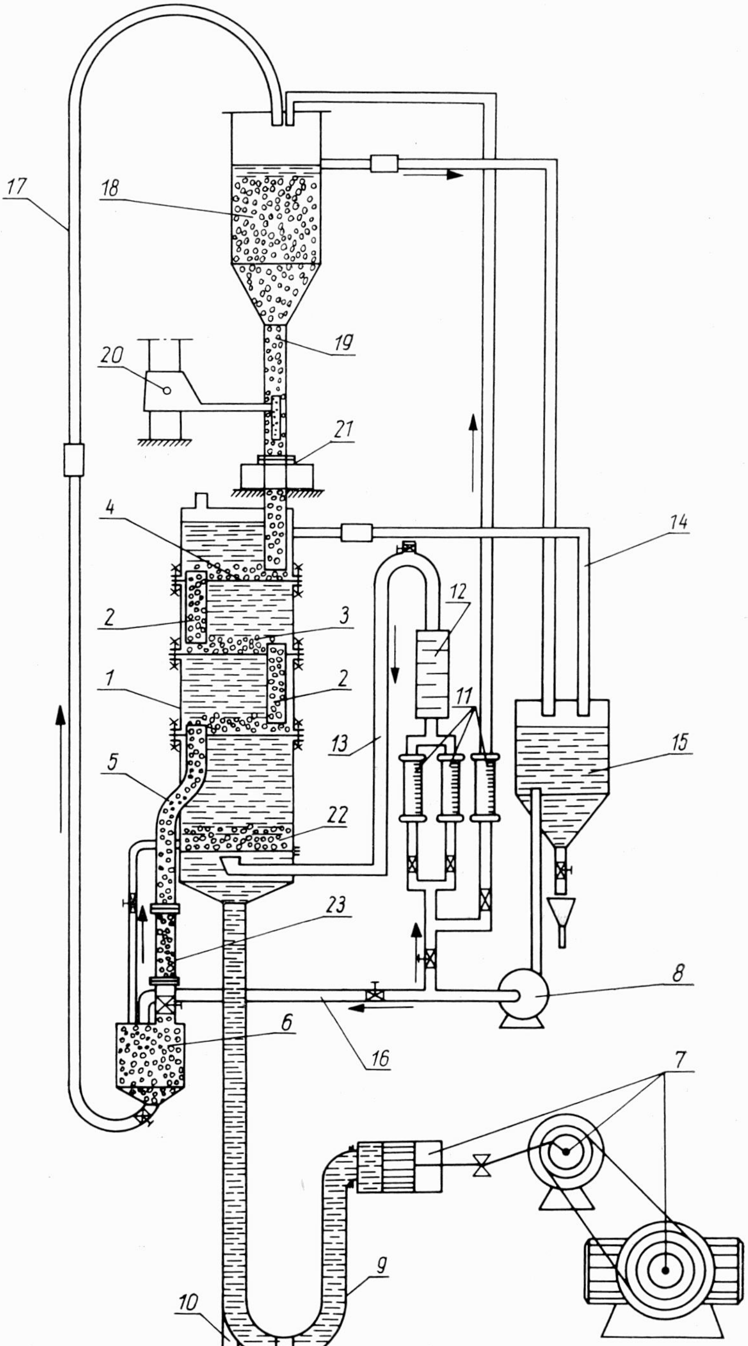
17
18
19
20
21
4
14
2
3
12
1
2
11
13
5
15
22
23
8
6
16
7
9
10

In view of the above the author's investigations have been confined to one basic problem. The purpose of the present research work was to explain the mechanism of the solid flow in the pulse column and — consequently — to formulate the equation permitting to design the above type of columns, taking into consideration the hydraulics of both solid and liquid flows.

2. EXPERIMENTAL APPARATUS

The research program has been realized on an experimental apparatus shown schematically in Fig. 2. Its basic part consisted of a vertical (137 × ×90 ×1290 mm) three-tray column (*1*), made of organic glass enabling visual observations of the process. The internal dimensions of the column cross-section amounted to 125 ×80 mm. The distance between the test trays being 210 mm. The main element of each tray was a wire net, the diameter of wire being 0.4 mm with mesches 0.85 ×0.65 mm. A part of the tray is occupied by a downcomer. Its special design permits to set the threshold and the immersion of the downcomer on arbitrary chosen heights, h and l, respectively. The lower part of the column, below the distributing tray (fourth from the top) was made of steel. The larger

---

Fig. 2. The scheme of the experimental apparatus
1 — vertical column, *2* — downcomers, *3* — fluidized granular material layer, *4* — wire network tray, *5* — outlet pipe for the solid, *6* — dispersed solid container, *7* — pulsator, *8* — pump, *9* — *U*-pipe, *10* — drainage, *11* — flow-meters, *12* — liquid antivibrator, *13* and *14* — inlet outlet pipes for the liquid, *15* — water container, *16* — pressure feeding pipe for the liquid, *17* — suspension pipe, *18* — suspension container, *19* — suspension feeding pipe, *20* — elevation pointer, *21* — micrometer screw, *22* — coarse-grained material layer, *23* — volumetric cell

Rys. 2. Schemat aparatury doświadczalnej
1 — kolumna pionowa, *2* — przelewy, *3* — sfluidyzowana warstwa materiału ziarnistego, *4* — półka kolumny wykonana z siatki drucianej, *5* — przewód odprowadzający ciało stałe z kolumny, *6* — zbiornik magazynujący ciało stałe, *7* — pulsator, *8* — pompa, *9* — połączenie *U*-rurowe, *10* — otwór spustowy cieczy, *11* — rotometry, *12* — tłumik drgań cieczy *13*, *14* — odpowiednio rura doprowadzająca i odprowadzająca ciecz z kolumny, *15* — zbiornik z wodą, *16* — przewód podający ciecz pod ciśnieniem *17* — przewód z zawiesiną ciała stałego w cieczy, *18* — zbiornik z zawiesiną ciała stałego w cieczy, *19* — rura dozująca zawiesinę, *20* — wskazówka do odczytu wysokości l (mm) *21* — śruba mikrometryczna, *22* — warstwa gruboziarnistego materiału, *23* — naczyńko pomiarowe $(\dot{m}_s)_{\max}$.

opposite walls of the apparatus, on the area limited by the 3rd tray and by the distributing fourth tray from the top has been additionally reinforced with special ribs. The above reinforcement appeared to be necessary because of the pressure exerted by the liquid subjected to pulsation. The *U*-pipe (made of vinylidene plastic) connecting the pulsator with the column and the stiffening of the lower part of this connection allowed to eliminate additional (harmful) vibrations transferred to the column from the working pulsator.

In the presented installation the following details are worth mentioning, namely:

a) a closed circulation of the liquid and of the solid allowing an economical solid and liquid disposal;

b) the application of a new type of feeder (Cf. Fig. 2 details *18*, *19*, *20*, *21*) — a simple patented divice [2] consisting of a solid storage bin (*18*), feeding pipe (*19*) and micrometer screw (*21*), lifting the pipe (*19*) above the upper tray to a given height this parameter being a decisive one in the mass flow rate of the solid, fed to the column;

c) the application of a vibration damper (*12*) in form of a chamber with partitions located alternately. This device produces an additional resistance and prevents the vibrations of the liquid to be transferred outside the column.

3. A SIMPLE MECHANISM OF THE SOLID FLOW DOWN THE TESTED COLUMN

The solid flow down a pulse column is closely related to fluidization process. All investigators dealing with such columns state that a semi-fluidized layer of the solid bed produced on the tray is due to the pulsing flow of the liquid.

Swinton and Weiss in [19] give one important detail. While writing about the abrasibility of the particles they point out that the abrasibility of the particles in pulse column is lower than in, e.g. a fluidization apparatus; since the fluidized bed is formed not continuously, but at time intervals. This statement suggests that the flow rate of the solid is not constant. More detailed observation of time solid moving along the tray and within the downcomer, performed at low pulsation frequency ($n = 115$ cycles/min) have fully confirmed this hypothesis.

The observations of the solid flow allowed to distinguish two stages depending on the position of the piston in the pulsator (Fig. 3). At the motion of the piston toward the inner dead centre (IDC), i.e. in the direction of the liquid flow, the bed from the downcomer gets to the tray, while a portion of granular material is leaving it (Fig. 3a). During the second stage, when the piston moves in the direction opposite to the

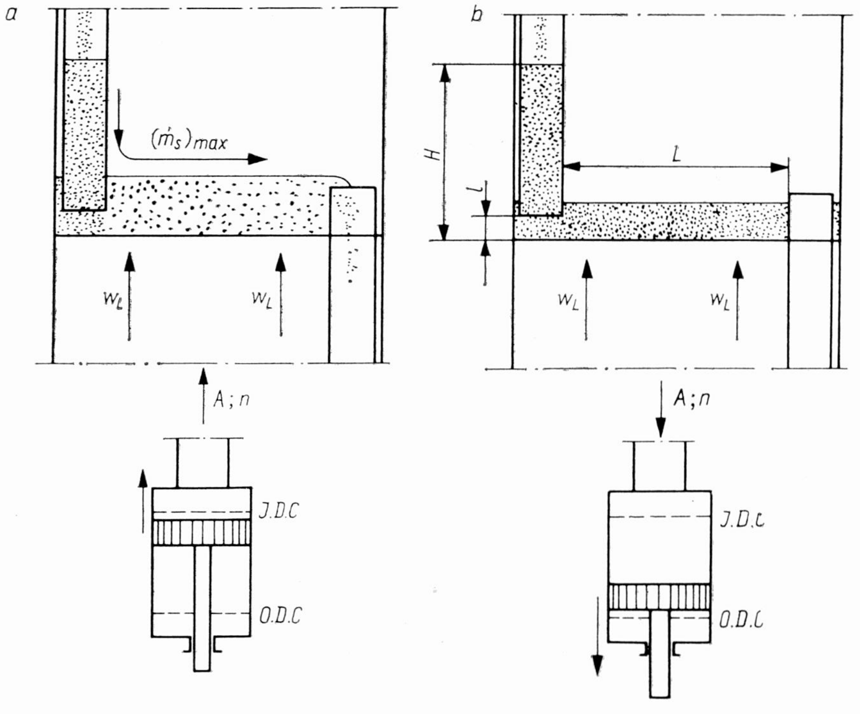

Fig. 3. Flow of the solid depending up on the position of the piston in the pulsator
a) I.D.C. – Inner Dead Centre
b) O.D.C. – Outer Dead Centre

Rys. 3. Przepływ ciała stałego w zależności od położenia tłoka w pulsatorze; a) przy ruchu tłoka do górnego martwego punktu, b) przy ruchu tłoka do dolnego martwego punktu

liquid flow (i.e. it moves toward the outer dead centre (O.D.C) the bed falls down the tray (Fig. 3b). Then the motion of the solid from the downcomer to the tray, and along the tray is stopped.

The flow of the solid presented above may be explained by the differences in the density of bed observed at operation periods of the column. The particles are closely "packed" in the downcomers and cannot move so freely as they do on the tray. Consequently, the liquid flow in the downcomers is strongly limited. Hence, it follows that the density of suspension in the downcomer does not depend on time. Without committing a remarkable error it may be assumed that

$$(\varrho_{sp}) \text{ of the downcomer} = (\varrho_{sp})_{\max} = \text{const}.$$

On the other hand, the density of the solid suspension on the tray vary with time, because of rhytmical vibrations performed by the bed layer, depending upon the position of the piston

$$(\varrho_{sp}) \text{ of the tray} = \varrho_{sp}(\tau).$$

It may be assumed, approximately, that the suspensions within the downcomer and on the tray will differ in density when the liquid velocity $w_l(\tau)$ is higher than the minimum fluidizing velocity w_{mf} (see Fig. 4).

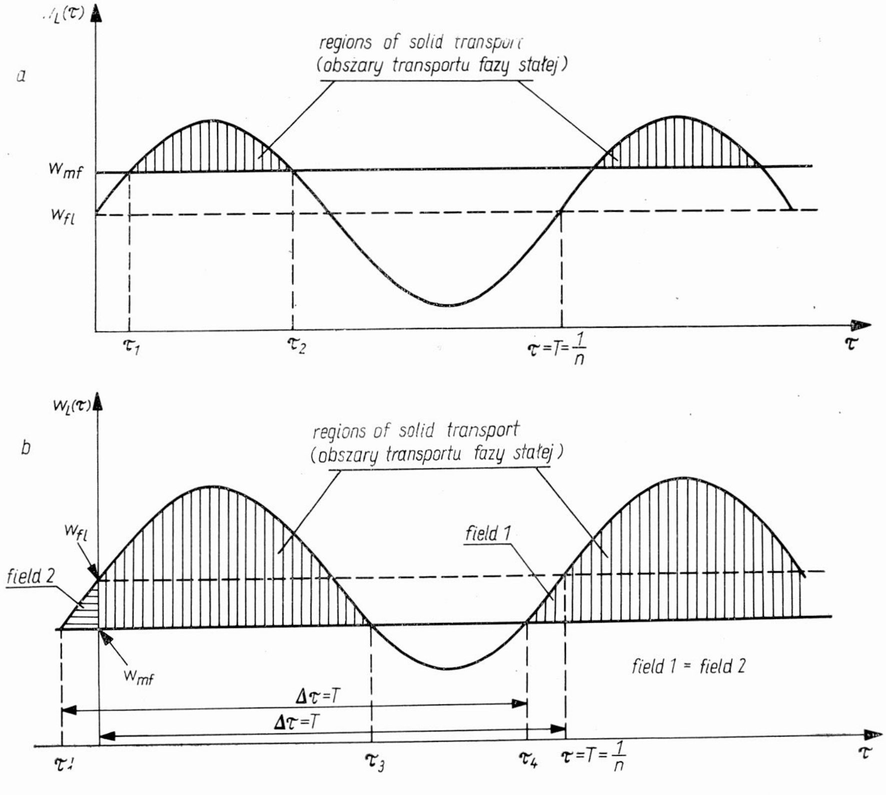

Fig. 4. Mechanism of the flow of the solid down the pulse column in cases a and b
Rys. 4. Mechanizm przepływu fazy stałej przez kolumnę pulsacyjną dla przypadku a i b;
a) $w_{fl} < w_{mf}$, b) $w_{fl} > w_{mf}$

Hence, the basic condition for the solid transport in the examined pulse column be written in form:

$$w_l(\tau) = w_{fl} + w_{\text{puls}} > w_{mf}. \tag{1}$$

The velocity of the liquid flow w_{fl} (marked in Fig. 4 by a dashed line) is constant, its value depends on the liquid flow rate. The second component of the liquid velocity w_{puls} related to the reciprocating motion of the pulsator is changing sinusoidally with time, and can be described by the equation

$$w_{\text{puls}} = \pi A n \sin(2\pi n \tau). \tag{2}$$

The eq. (2) results from the crank mechanism [8, 14]. Thus, if

$$w_l(\tau) = w_{fl} + \pi A n \sin(2\pi n \tau) > w_{mf} \tag{3}$$

then

$$(\varrho_{sp})_{\text{downc.}} = (\varrho_{sp})_{\max} > (\varrho_{sp})_{\text{tray}} = \varrho_{sp}(\tau). \tag{4}$$

The solution of the inequality (3) allows to determine the time intervals for the solid flow (hatched area in Fig. 4), namely:

for case I: $w_{fl} < w_{mf}$ — the time interval $(\tau_1 - \tau_2)$

for case II: $w_{fl} > w_{mf}$ — the time interval $(0 - \tau_3) + (\tau_4 - T) = \tau_1 - \tau_3$ (see Fig. 4).

From (3) it follows, moreover, that there exists a gradient between the momentary $w_l(\tau)$ and minimum w_{mf} velocities of liquid flow

$$\Delta w_l(\tau) = w_{fl} + w_{\text{puls}} - w_{mf} > 0. \tag{5}$$

The difference in velocity $\Delta w_l(\tau)$ yields the difference in the porosity on the tray $\Delta\varepsilon(\tau)$ which, in turn, brings about the difference in the density on the tray

$$\Delta w_l(\tau) \longrightarrow \Delta\varepsilon(\tau) \longrightarrow \Delta\varrho_{sp}(\tau) = (\varrho_{sp})_{\max} - \varrho_{sp}(\tau). \quad (6$$

Finally, the gradient of density (between the suspension on the tray and in the downcomer) allows the granular material to be shifted along the tray, i.e.

$$(\dot{m}_s)_{\max} > 0. \tag{7}$$

It is known that

$$(\varrho_{sp})_{\max} = (1 - \varepsilon_{\min}) \cdot \varrho_s + \varepsilon_{\min} \cdot \varrho_c, \tag{8}$$

$$\varrho_{sp}(\tau) = (1 - \varepsilon(\tau)) \cdot \varrho_s + \varepsilon(\tau) \cdot \varrho_c. \tag{9}$$

By introducing the basic relations (8) and (9) into equation (6) we get

$$\Delta\varrho_{sp}\ (\tau) = (\varepsilon(\tau) - \varepsilon_{\min})\cdot(\varrho_s - \varrho_c), \tag{10}$$

where

$$\varepsilon(\tau) = f(w_l(\tau)) = f(w_{fl} + \pi A n \sin(2\pi n\tau)). \tag{11}$$

Let us suppose that the function (11) is known. With this assumption the mass solid flow at an arbitrary moment is proportional to the temporary density difference, i.e.

$$dm_s \sim d(\Delta\varrho_{sp}(\tau)), \tag{12}$$

$$dm_s = V_{sp} d(\Delta\varrho_{sp}(\tau)). \tag{13}$$

Assumming approximately that V_{sp}, m^3, is time independent, the integration of the equation (13) yields the mass flowing down the apparatus during the time ranging from 0 to T, where $T = 1/n$.

$$\int_{m_{s_1}}^{m_{s_2}} dm_s = V_{sp} \int_{\tau_1,(\tau_1')}^{\tau_2,(\tau_3)} \Delta\varrho_{sp}(\tau)\,d\tau \tag{14}$$

and, finally

$$m_s = m_{s_2} - m_{s_1} = V_{sp}(\Delta\varrho_{sp})_a, \tag{15}$$

where

$$(\Delta\varrho_{sp})_a = \frac{\int_{\tau_1,\tau_1'}^{\tau_2,\tau_3} \Delta\varrho_{sp}(\tau)\,d\tau}{\Delta\tau}. \tag{16}$$

Dividing both sides of the equation (15) by T and denoting m_s/T by $\dot{m}_s$ we get:

$$\dot{m}_s = V_{sp}\frac{1}{T}(\Delta\varrho_{sp})_a. \tag{17}$$

At the solid flow rate over, which the downcomer is fulfilled, i.e. if the hight H of the bed in the downcomer (Fig. 3) is sufficiently great, then

$$(\varrho_{sp})_{\text{downc.}} = (\varrho_{sp})_{\max}$$

and

$$\dot{m}_s = (\dot{m}_s)_{\max}.$$

finally,

$$(\dot{m}_s)_{\max} = V_{sp} \cdot n \cdot (\Delta \varrho_{sp})_a \tag{18}$$

So far, however, the relation (11) has not been sufficiently defined. Although the behaviour of a single particle in the pulsing field is determined, only a few data on the whole bed behaviour may be found in the cited literature.

For this reason it seemed necessary to simplify the relation (11) by normalizing the time varying liquid flow rate, since for the uniform flow of the liquid the relations between its porosity and velocity are known. To this end the momentary velocity of the liquid has been substituted by an average velocity (integral mean), the latter value being characteristic of the momentary velocity $w_l(\tau)$ within the range of granular solid transport. Hence, the average velocity $(w_l)_a$ is equal to

$$(w_l)_a = \frac{\int\limits_{\tau_1,\tau_1'}^{\tau_2,\tau_3} (w_{fl} + \pi A n \sin(2\pi n \tau)\, d\tau}{\Delta\tau}$$

$$= w_{fl} + \frac{A(\cos(2\pi n \tau_1)^{(\tau_1')} - \cos(2\pi n \tau_2^{(\tau_3)}))}{2\Delta\tau}. \tag{19}$$

The velocity $(w_l)_a$ being known, and in view of the simplified equation of Zaki-Richardson, the mean porosity may be determined

$$\varepsilon_a = \left(\frac{(w_l)_a}{w_t}\right)^{1/x}, \tag{20}$$

where

$$x = \frac{\lg\left(\frac{w_{mf}}{w_t}\right)}{\lg \varepsilon_{mf}}. \tag{21}$$

Let now the momentary porosity $\varepsilon(\tau)$ in eq. (10) be substituted by the ε_a. We get

$$(\Delta\bar{\varrho}_{sp})_a = (\varepsilon_a - \varepsilon_{\min})(\varrho_s - \varrho_c). \tag{22}$$

Substituting $(\Delta\varrho_{sp})_a$ in formula (17) by $(\Delta\bar{\varrho}_{sp})_a$ we get

$$(\dot{m}_s)_{\max} = V_{sp}\cdot n\cdot(\Delta\bar{\varrho}_{sp})_a. \tag{23}$$

The constant $V_{sp}(m^3)$ when defined physically is the volume of the suspension that moves along the tray during one cycle. It has been shown experimentally that

$$V_{sp} = C_L\cdot F_r \tag{24}$$

C_L is a constant, m,
$F_r = a\cdot l_2$ (see Fig. 5, details in [3]).

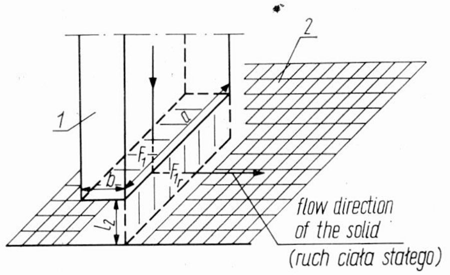

Fig. 5. Graphical illustration of F_1 and F_{1r} areas
1 – downcomer, 2 – wire network tray
$F = a\cdot b$, $F_{1r} = a\cdot l_2$
Rys. 5. Graficzna ilustracja powierzchni F_1 i F_{1r}
1 – przelew, 2 – półka wykonana z siatki drucianej

Thus, the final relation may be written in form

$$(\dot{m}_s)_{\max} = C_L\cdot F_r\cdot n\cdot(\Delta\bar{\varrho}_{sp})_a. \tag{25}$$

This equation allows to find out the maximum mass flow of the solid which may be transported by a tray under the given working conditions. The mean density difference (by analogy to the modelling method used in chemical engineering) can be considered as the driving force of the solid flow.

For any measuring point satisfying the relation (25) the values: $(\dot{m}_s)_{\max}$, F_r, n and $(\Delta\bar{\varrho}_{sp})_a$ may be determined experimentally. Hence, the value of the constant C_L (in meters) may be also determined. According to the assumed model this constant (coefficient) may be defined physically. Its value is given by the distance covered by the granular material moving along the tray in time corresponding to one cycle of the pulsator. The front surface of the shifted solid is denoted by F_r. More detailed information on the measurements of the separate values occuring in final relation (25) is given in [3].

4. CORRELATION OF THE VALUE C_L

It has been shown that the value C_L can be determined from eq. (25) for an arbitrary measuring point. Nevertheless, C_L being a factor deciding on the shift of the solid along the tray — is not supposed to be identical for all measurements. This hypothesis has been confirmed by the analysis of the obtained results. It has been stated that the values of C_L are related to $(\dot{m}_s)_{\max}$ and pulsation frequency by direct and inverse proportions, respectively.

From the fact that the solid flow rate grows with the increasing frequency of pulsation and C_L value it may be inferred that the $(\dot{m}_s)_{\max}$ value does not depend on C_L, but on the product $(n \cdot C_L)$. The latter is

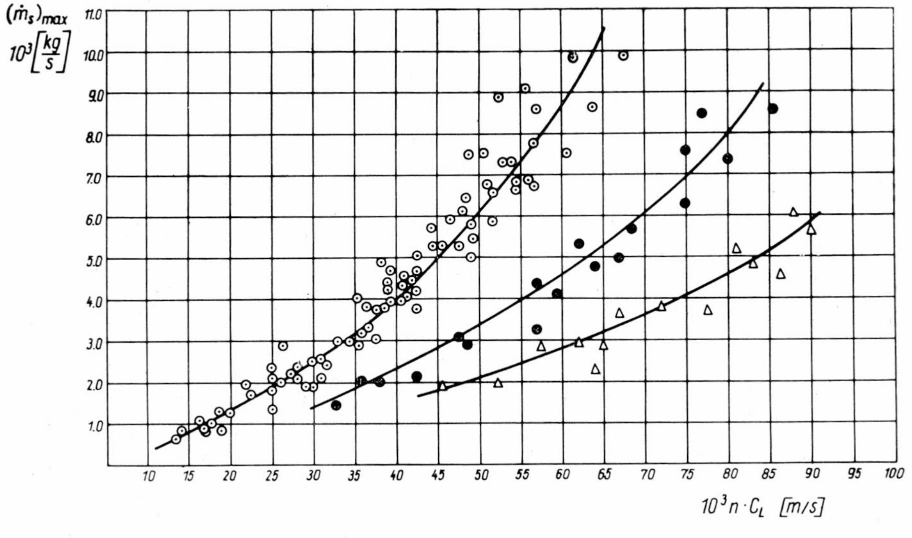

Fig. 6. The maximum rate $(\dot{m}_s)_{\max}$ versus the shift velocity $n \cdot C_L$, given for the system: sand (d_p = 1.75 mm) — water

⊙ — at downcomer cross-section of F_1 = 586 mm²
● — ,, ,, F_1 = 398 mm²
△ — ,, ,, F_1 = 256 mm²

Rys. 6. Zależność natężenia przepływu $(\dot{m}_s)_{\max}$ od prędkości przesuwu $n \cdot C_L$ na przykładzie układu: piasek (d_z = 1,75 mm) — woda

⊙ — przy powierzchni poprzecznej przelewu F_1 = 586 mm²
● — ,, ,, F_1 = 398 mm²
△ — ,, ,, F_1 = 256 mm²

considered to be the mean velocity at which the granular material is shifted along the tray. The effects exerted by $n \cdot C_L$ and cross-section area of the downcomer on the value of $(\dot{m}_s)_{max}$ are shown in Fig. 6. The measurements performed for the systems: sand ($d_p = 1.75$ mm) — water/glycerine solution have allowed to present the obtained results graphically (Fig. 6). Three curves presented in this Figure have been obtained for different areas (F_1) of the examined downcomer. A more detailed ana-

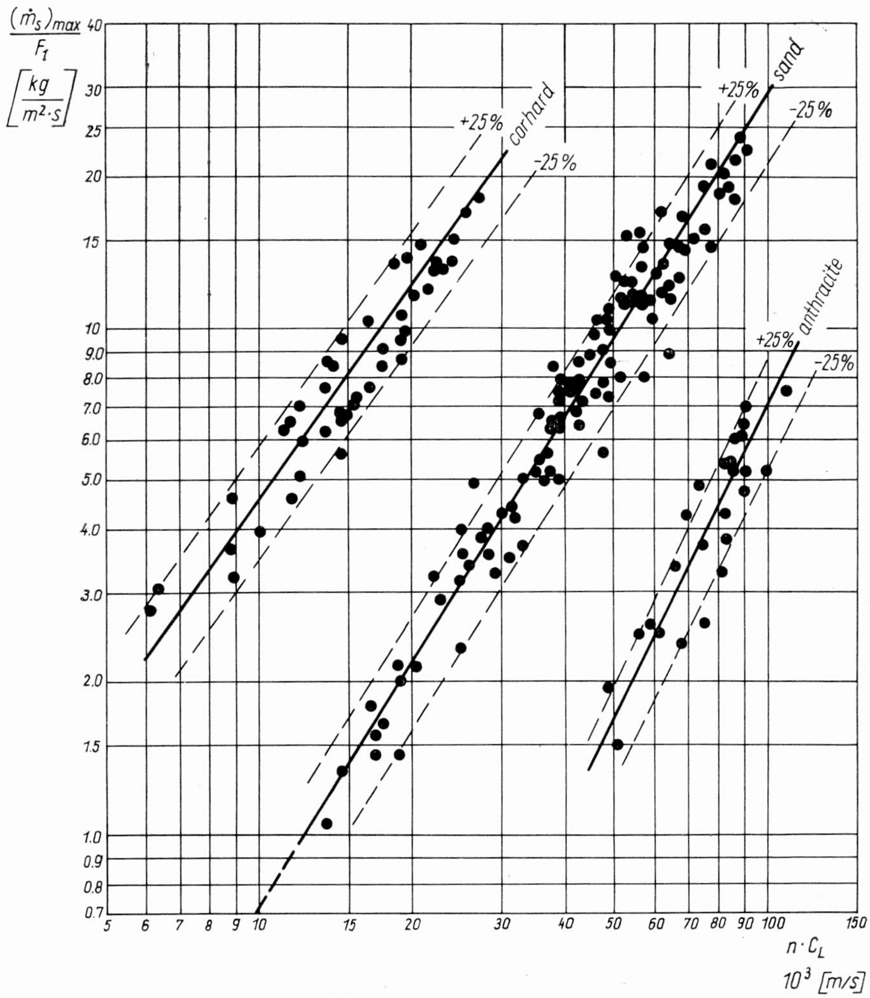

Fig. 7. The relationship between $(\dot{m}_s)_{max}/F_1$ and $n \cdot C_L$

Rys. 7. Zależność między $(\dot{m}_s)_{max}/F_1$ i $n \cdot C_L$

lysis has shown that for a $((\dot{m}_s)_{max}/F_1)$ is closely related to the product $n \cdot C_L$. In double logarithmical system

$$\frac{(\dot{m}_s)_{max}}{F_1} = f(n \cdot C_L)$$

is a straight line (Fig. 7). Thus it may be described by the power function

$$\frac{(\dot{m}_s)_{max}}{F_1} = z \cdot (n \cdot C_L)^v. \tag{27}$$

For the three examined materials, i.e. anthracite, sand and cohard, (their densities z being equal to 1.525, 2.620 and 3.750 kg/m³, respectively) three, approximately parallel straight lines have been obtained. Because of a slight divergence in the value of the exponent u its geometrical mean has been assumed. For the examined material

$$u_a = 1.65.$$

The constant z in eq. (27) is more complex one, being not a straight line even in a double logarithmic system. Therefore it seems advisable to determine its value from the diagram (Fig. 8).

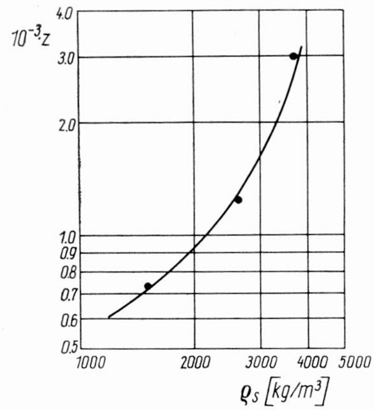

Fig. 8. The value of constant z versus the density of the granular material ϱ_s

Rys. 8. Zależność stałej z od gęstości właściwej ziarnistego materiału ϱ_s

Finally, an additional equation for the relationship between the mean velocity of the shift of granular material along the tray and its maximum mass rate has been obtained

$$\frac{(\dot{m}_s)_{max}}{F} = z \cdot (n \cdot C_L)^{1.65}, \tag{28}$$

where from Fig. 8.

$$z = f(\varrho_s). \tag{29}$$

5. THE ARGUMENTS JUSTIFYING THE ASSUMED MODEL OF THE SOLID FLOW

It might appear that, contrary to our assumption, the flow of granular material should depend on the accelerations and the energy of pulsation, rather than on the total velocity of the liquid. The facts presented below speak, however, for the model assumed.

The analysis of the effect of the product An on the solid rate $(\dot{m}_s)_{\max}$ allowed to state that the relation between the both values was approximately proportional (see Fig. 9). On the other hand $w_{\text{puls}} = \pi A n \sin(2\pi n \tau)$.

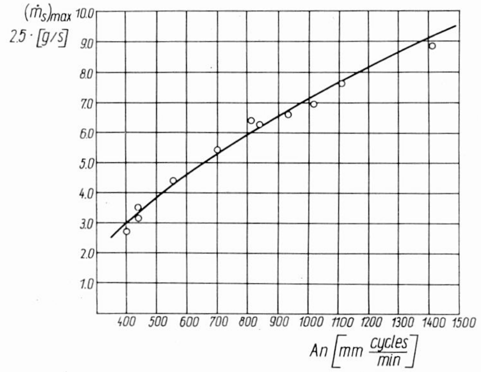

Fig. 9. Relationship between $(\dot{m}_s)_{\max}$ and the product $A \cdot n$
System: anthracite ($d_p = 1.75$ mm) — water, $l_2 = 5.0$ mm, $\dot{v}_c = 53.9 \pm 3.0$ (l/h)
Rys. 9. Zależność między natężeniem $(\dot{m}_s)_{\max}$ a iloczynem $A \cdot n$
Układ: antracyt ($d_z = 1{,}75$ mm) — woda, $l_2 = 5{,}0$ mm; $\dot{v}_c = 53{,}9 \pm 3{,}0$ (l/h)

Hence, it follows that the rate $(\dot{m}_s)_{\max}$ is proportional to the pulse velocity of the liquid, is not related to the acceleration or the energy of pulsation which depend on A^1n^2, and A^2n^3, respectively.

To verify the assumed model the values of the minimum fluidizing velocity, obtained from our experiments and from the calculations, based on the well-known Ergun and McLeva formulas have been compared. The method by which the authors have determined the minimum fluidizing velocity values, further called, "the method of graphical extrapolation", has been based on the fundamental assumption of the suggested model; according to this model the solid moves if the sum of fluid velocities is greater than the minimum fluidizing velocity i.e. if

$$w_1(\tau) = w_{fl} + w_{\text{puls}} > w_{mf}$$

then

$$(\dot{m}_s)_{\max} > 0.$$

This assumption leads to the next conclusion, namely that if

$$w_1(\tau) = w_{fl} + w_{\text{puls}} = w_{mf}$$

then

$$(\dot{m}_s)_{\max} = 0.$$

Thus, by extrapolation to zero of the results obtained for $(\dot{m}_s)_{\max}$ in system of coordinates

$$(\dot{m}_s)_{\max} = f(w_{fl} + (w_{\text{puls}})_a)$$

the value of w_{mf} is given by the abscissa. Since during one cycle $T = 1/n$ the liquid in the column covers the distance $2A$

$$(w_{\text{puls}})_a = 2An.$$

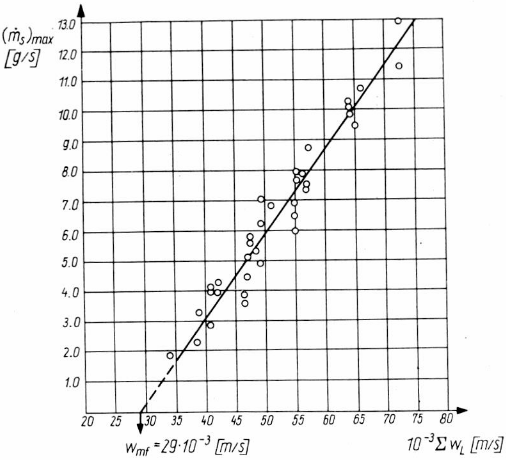

Fig. 10. Determination of w_{mf} by graphical extrapolation method System: corhard ($d_p = 1.75$ mm) – water, $l_2 = 10$ mm, $F_{1r} = 528$ mm^2 $\Sigma w_c = w_{fl} + (w_{\text{puls}})_a$

Rys. 10. Wyznaczenie prędkości w_{mf} metodą ekstrapolacji graficznej. Układ: corhard ($d_z = 1{,}75$ mm) – woda, $l_2 = 10$ mm, $F_{1r} = 528$ mm^2

An example of determination of w_{mf} by extrapolation of $(\dot{m}_s)_{\max}$ to zero is shown in Fig. 10.

The values of w_{mf} obtained by graphical extrapolations and by from the Ergun and McLeva equations are shown in Table

The values of w_{mf} obtained for the systems investigated (liquid—solid; $d_p = 1.75$ m)

Wartości w_{mf} dla badanego układu ciecz — ciało stałe, $d_p = 1{,}75$ m.

System	Values of w_{mf} 10^3 m/s, determined			
	By graphical extrapolation		From the equations	
	Determined values	Average	Ergun's	Mc Leva's
Sand — Water $d_p = 1.75$ mm	21.5 ; 20.5 19.5 ; 21.5 21.5 ; 21.5	21.0	19.8	18.0
Santhracite — Water $d_p = 1.75$ mm	7.5 ; 8.5	8.0	8.4	7.8
Corhard — Water $d_p = 1.75$ mm	29.0 ; 29.0	29.0	32.3	29.0
Sand — Glycerine $d_p = 1.75$ mm $6.91 \cdot 10^{-3}$ N·s/m²	5.5 ; 4.5	5.0	4.2	3.3

It is easy seen that values of minimum fluidizing velocity determined by the three methods do not differ significantly. Thus in view of the graphical extrapolation (based on the author's experimental data) for the model discussed prove to be true.

The assumption of the above model may be also justified by some statements given by Slater in [17]. According to Slater the bed porosity in pulse columns is to be calculated from the relation

$$w_{\text{puls}} + w_{fl} = 0.015 \cdot \varepsilon^2. \tag{31}$$

Slater, like the authors of the present paper, made use of a simplified Zaki-Richardson equation, by adjusting it to pulsing flow of the liquid. He assumed that both components of the liquid flow namely w_{fl} and w_{puls} are additive. This assumption corresponds to the simplification taken for the model, described by the equation (19) in which $(w_l)_a$ is the sum of the both components. Hence, the equation (31) is a transformation of the eq. (20). The differences occur only in the values of the used constants. The method by which the both constants (preceding the porosity ε

and its power index) have been calculated in the model assumed seems to be more adequate. It is difficult to expect the validity of the eq. (31) within a sufficiently wide range of density and size of the particles.

CONCLUSIONS

The available literature does not provide the reader with a full analysis of solid flow down a vertical pulse column. The purpose of the present paper was to explain this process. The model presented has been based on the assumption that the motion of solid induces the differences in the density of suspensions within downcomer and on the tray and that this difference is closely related to fluidization. In view of the results obtained from the author's own investigations the product $(n \cdot C_L)$ occurring in the eq. (25) has been correlated with $(\dot{m}_s)_{\max}$. The obtained relationship (27) is satisfied for the variables ranging within the following values:

$An = 200-2050$ mm/min, $l = 5-12.5$ mm,
where $A = 0.9-10.2$ mm, $\varrho_s = 1525-3750$ kg/m³,
$n = 160-275$ cycle/min $\varrho_c = 1.000-1.100$ kg/m³,
$w_{fl} = (3.0-30)\cdot 10^{-3}$ m/s $\eta_c = (1.0-6.9)\cdot 10^{-3}$ N·s/m².

The arguments speaking for the model of the solid flow discussed in the present paper have been given. It should be emphasized that the whole problem being much complicated. The model presented simplifies the mechanism of solid flow down the columns of the assumed type. Therefore further investigations on this problem seem to be necessary.

MECHANIZM PRZEPŁYWU ZIARNISTEJ FAZY STAŁEJ W PIONOWEJ KOLUMNIE PULSACYJNEJ DLA UKŁADU: CIECZ–CIAŁO STAŁE

W pracy przedstawiono aparaturę do ciągłego przeciwprądowego transportu ciała stałego i cieczy, pracującą na zasadzie przepływu pulsacyjnego. Równania opisujące ten model przepływu zostały potwierdzone przez wyniki uzyskane z doświadczeń przeprowadzonych w skali półtechnicznej.

Z badań uzyskano dodatkowo zależność empiryczną między średnią szybkością przesuwu cząstek $(n \cdot C_l)$ i natężeniem przepływu masy ziarnistego ciała stałego $(\dot{m}s)_{\max}$. Podano także argumenty przemawiające za przyjętym modelem. W celu uniknięcia wpływu ubocznych czynników na przebieg badanego zjawiska w doświadczeniach zastosowano układy modelowe, których komponenty były chemicznie obojętne oraz nie wykazywały tendencji do aglomeracji i rozpuszczania.

DURCHFLUSSMECHANISMUS DER KÖRNIGEN FESTEN PHASE IN DER SENKRECHTEN PULSIERENDEN KOLONNE FÜR DAS SYSTEM: FLÜSSIGKEIT – FESTER STOFF

In der Arbeit wurde die Apparatur für die kontinuierliche Gegenstrombeförderung von festen Stoffen und Flüssigkeiten dargestellt, die nach dem Prinzip des pulsierenden Durchflusses arbeitet. Die Gleichungen, die dieses Durchflussmodell beschreiben, wurden durch die bei den in halbtechnischem Masstab durchgeführten Experimenten erzielten Ergebnissen bestätigt.

Bei den Untersuchungen wurde zusätzlich die empirische Abhängigkeit zwischen der Schubgeschwindigkeit der Teilchen ($n \cdot C_1$) und dem Mengenstrom der körnigen Masse des festen Stoffes $(M_s)_{\max}$ erlangt. Es wurden auch die Argumente angegeben, die für das angenommene Modell sprechen. Um den Einfluss von Nebenerscheiningen auf den Verlauf des untersuchten Vorgangs auszuschliessen wurden bei den Versuchen Modellsysteme angewandt, deren Komponente in chemischer Hinsicht neutral waren und keine Tendenz zu Agglomeration und Auflösung aufwiesen.

МЕХАНИЗМ ПРОТЕКАНИЯ ТВЕРДОЙ ЗЕРНИСТОЙ ФАЗЫ В ПУЛЬСИРУЮЩЕЙ ВЕРТИКАЛЬНОЙ КОЛОНКЕ ДЛЯ СИСТЕМ ЖИДКОСТЬ – ТВЕРДОЕ ТЕЛО

Описана аппаратура для непрерывного противоточного транспорта твердого тела в жидкости, работающая по принципу пульсирующего течения. Уравнения, описывающие эту модель течения, были подтверждены результатами, полученными от опытов, произведенных в полутехническом масштабе.

В ходе исследований была добавочно определена эмпирическая зависимость между средней скоростью перемещения частиц и интенсивностью течения зернистой массы твердого тела $(M_s)_{\max}$. Приведены также аргументы в пользу принятой модели. Во избежание влияния побочных факторов на ход исследуемого явления применялись при испытаниях модельные системы, компоненты которых были нейтральными в химическом отношении; в них не обнаруживались, кроме того, тенденции к агломерированию и растворению.

REFERENCES

[1] Brown B. B., *Jednostki operacyjne* (transl. from English), Warszawe 1960, p. 236–240.

[2] Firewicz H. and Koch R., Polish patent 64726 (1972), 21$^{\text{th}}$ Jan. 1970 Appl.

[3] Firewicz H., *Hydraulics of a vertical pulse column for systems: liquid-solid*, Dissertation. Technical University of Wrocław, Wrocław 1973.

[4] Grimmett E. S.; USA patent 3, 116, 980 (1964), 27$^{\text{th}}$ March 1961 Appl.

[5] Grimmett E. S.; and Brown B., Ind. Eng. Chem. (1962), **54/11**, 24–28.

[6] Hiester N. K., Phillips R. C.; Chem. Engng (1954), **61**, 161–180.

[7] Koch R. and Firewicz H., Nowa Technika 85 (1969), 143–194.

[8] Krakowski J. et al., *Maszynoznawstwo chemiczne,* WNT, Warszawa 1960, 108–111.
[9] Kunii D., Levenspiel O., *Fluidization Engineering,* New York-London-Sydney-Toronto 1969, John Wiley and Sons, p. 63–73.
[10] Leva M., *Psevdoozhizheniye* (transl. from English) 1969, p. 33 and 101–118.
[11] Minty D. W. et al., Austr. J. Appl. Sci (1953), **4**, 530–542.
[12] Mc Neill R., Swinton E. A., Weiss D. E., Journal of Metals (1955) **7**, 912–921.
[13] Pettyjohn E. S., Christiansen E. B., Chem. Eng. Progr. (1948), **44**, 157.
[14] Pikoń J., *Maszynoznawstwo i technika cieplna,* part IV – *Elementy maszyn,* Gliwice 1969, 112–120.
[15] Rickles R. N.; Chem. Engng March (1965), **58**. 1, 157–172.
[16] Slater M. J., Brit. Chem. Engng (1969), **14**, 1, 41–46.
[17] Slater M. J., Ion Exch. Process Ind. Pap. Conf. (1969), publ. 1970, 127–132.
[18] Swinton E. A. and Weiss D. E.; Austr. J. Appl. Sci (1953), **4**, 316–328.
[19] Weiss D. E. and Swinton E. A.; USA patent 2. 742, 381 (1956), 10th Sept, 1952 Appl.
[20] Wen C. Y. and Yu Y. H.; A. J.Ch.E.J. (1966), **12**, 610–612.
[21] Zenz F. A. and Othmer D. F., *Fluidization and Fluid-Particle Systems,* New York 1960, Reinhold Publishing Corporation, p. 109, 230–257.